Effect of Load on Active Friction Control using Ultrasonic Vibrations

Shravan Bharadwaj, Marcelo J. Dapino
Smart Vehicle Concepts Center, Department of Mechanical Engineering, The Ohio State University, Columbus, OH 43210 USA

ABSTRACT

[Smart Vehicle Workshop] The ability to control the effective friction coefficient between sliding surfaces is of particular fundamental and technological interest for automotive applications. It has been shown that the friction force between sliding surfaces can be reduced by superimposing ultrasonic vibrations on the macroscopic sliding velocity. We developed a systematic approach based on experiments and models to describe and characterize the friction force between sliding surfaces in the presence of ultrasonic vibrations generated by a piezoelectric transducer. The controlling parameters in this study are static contact pressure, relative velocity, voltage, and frequency. Using a low power PMN-PT driver, we experimentally demonstrate a decrease of up to 68 % in effective friction coefficient and analytically show the underlying principle behind the friction reduction. The trends show a decrease in the effect with increasing sliding velocity and normal load. The results underscore the role of ultrasonic power in harnessing the friction control concept in applications.

Keywords: Sliding friction, Coulomb, ultrasonic vibrations, active control, piezoelectric actuator

1. INTRODUCTION

Friction is the resistance to motion during sliding or rolling that is experienced when one solid body moves tangentially over another with which it is in contact. There are two main types of friction that are commonly encountered: dry friction or "Coulomb" friction and viscous friction. Dry friction is the tangential component of the contact force that exists when two solids in contact move relative to one another. The tangential force required to initiate motion (static friction force) is greater than or equal to the tangential force required to maintain relative motion (kinetic friction force) [1].

Friction is not a material property; it is a system response. Amonton [2] proposed laws of friction for macroscopic bodies in contact, which state, 1) friction force is directly proportional to the applied load, and 2) friction force is independent of the apparent area of contact. Coulomb later added a third law, stating that the dynamic friction is independent of the sliding velocity [1]. However, at a microscopic level, these friction laws do not necessarily hold. At these scales, adhesion plays an important role and frictional forces depend on the contact area.

Friction control in the presence of ultrasonic oscillations has been reported in the literature. One way of reducing friction is by superimposing longitudinal or perpendicular vibrations on macroscopic motion [3-5]. Coulomb's friction laws have been shown to be applicable while modeling contact mechanics in ultrasonic applications [3], [4]. Energy considerations have been used to show that a significant reduction in friction can be attained with little additional energy to the system [5]. Recently, it was demonstrated using numerical analysis that Dahl's friction model is more appropriate while modeling friction reduction in the presence of superimposed longitudinal vibrations [6]. The application of ultrasonics to actively modulate friction coefficients can be utilized in various vehicle systems (e.g., gear trains, sliding door/window mechanisms, seat belt systems, engine cylinders, brake systems, etc.), which often present contradicting requirements between sliding velocity, tangential and normal forces, and heat dissipation due to frictional effects.

Superposition of high-frequency vibrations on low-frequency disturbances or dither control has been proposed for suppressing squeal in automotive brake systems [7-9]. It has been shown that there is a reduction in friction between the brake pad and rotor due to the application of a normal dither signal [8], [9]. However, introduction of normal dither signals causes a small reduction in the braking torque (<2%) [9]. Active or "smart pads" have been developed [10] which

Further author information: (Send correspondence to M.J.D.)

M.J.D.: E-mail: dapino.1@osu.edu, Telephone: 1 614 688 3689
S.B. : E-mail: bharadwaj.4@osu.edu, Telephone: 1 614 247 7480

Industrial and Commercial Applications of Smart Structures Technologies 2009,
edited by Benjamin K. Henderson, M. Brett McMickell, Proc. of SPIE Vol. 7290, 72900G
 · doi: 10.1117/12.817052

include embedded piezoelectric elements between the brake pad material and the metallic backing plate to generate a normal harmonic force. This force provides a small variation about the mean clamping force. Tangential dither influences the friction force due to its averaging effect whereas normal dither changes the mean friction coefficient. In general, tangential dither is more effective than normal dither in stabilizing a system having self-excited oscillations arising from Stribeck friction [11].

This paper aims to characterize the behavior of sliding friction in the presence of ultrasonic vibrations superimposed longitudinally in the direction of motion. By correlating data from experiments conducted to measure the reduction in friction force with Coulomb and Dahl friction models, we analyze the dependence of this phenomenon on various controlling parameters such as static contact pressure, relative velocity, voltage and frequency.

2. EXPERIMENTS

The ultrasonic transducer employed in this study is a hollow PMN-PT (Lead Magnesium Niobium- Lead Titanate) stack manufactured by EDO Corporation. The stack is placed between two aluminum shells and preloaded by a #6-32 through bolt and Bellville washers. Following the design of Littmann et al. [3], conical waveguides were attached at each end of the bolt (Fig. 1). This stack requires an optimum preload of 500-600 N. The ends of the transducer remain the points of contact with the base surface during the experiment. Since the washers are an order of magnitude stiffer than the bolt, most of the stack's displacement is transmitted to the shells.

Table 1 shows the specifications of the transducer. When placed on an inclined guide rail, the transducer remains at rest due to the friction force acting at the contact points. Upon application of a sinusoidal voltage (1 V to 10 V) at ultrasonic frequencies (20 kHz to 60 kHz), the transducer slides down the guide rail. In the presence of ultrasonic oscillations superimposed on the macroscopic motion of the transducer, a reduction in friction is measured. The amount of friction reduction depends on the voltage, frequency, preload and the velocity ratio (ξ). The velocity ratio is defined as the ratio of the macroscopic velocity of the transducer ($v_{transducer}$) to the velocity of the ultrasonic vibrations ($v_{vibration}$).

Fig.1. PMN-PT stack ultrasonic transducer.

Table 1. Transducer specifications.	
Material Specification of Stack	Edo Corp. PMN-PT Stack
Number of discs in stack, n	62
d_{33} of PMN-PT	730 x 10^{-12} m
Required displacement, ΔL	0.7 x 10^{-6} m
Voltage (maximum), V_{max}	$\Delta L/(d_{33} \times n)$ = 15.466 V
Frequency, f	60 kHz
Preload, F	150 lbs = 670 N
Capacitance, C	300 nF
Current (maximum), I_{max}	$2\pi fCV_{max}$ = 1.75 Amps
Impedance, Z	$1/C\omega$ = 8.84 Ω
Stiffness of stack, K_{stack}	3.14 x 10^{8} N/m
Stiffness of bolt, K_{bolt}	3.7 x 10^{7} N/m
Deflection in stack due to preload, ΔL_{stack}	F/K_{stack} = 2.133 μm
Nominal displacement of stack, ΔL_0	36 μm
Maximum displacement possible, ΔL	ΔL_0 (K_{stack}/ (Kstack + K_{bolt})) = 32.2 μm

An experimental apparatus similar to the one developed by Littmann et al. [3] was designed as shown in Fig. 2. A pneumatic cylinder pushes an aluminum slider carriage at different velocities. The slider carriage slides on aluminum guide rails. The ultrasonic transducer is attached to the carriage at one end. The ends of the transducer remain in contact with the guide rail surface throughout the tests.

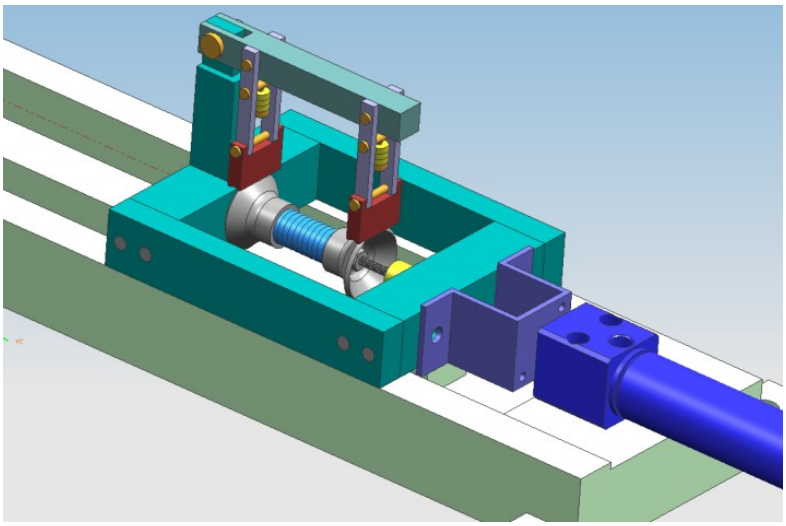

Fig.2. Rendering of friction control experimental setup.

An adapter bracket connects one end of the transducer (#6-32 bolt) to the (¼ - 28) hole of a load cell (MPL-50-T). The load cell measures the average frictional force at the contact interface as the transducer moves. The function of the slider carriage is to transfer motion from the pneumatic actuator to the transducer. The carriage consists of a lever arm designed to apply external load on the transducer. Adjusting the flow of air into the cylinder controls the macroscopic velocity of the carriage and transducer. For these tests, the voltage/frequency of excitation is set at 6 V peak-to-peak, at 40 kHz. At this frequency, the transducer operates in half wavelength mode and the maximum deformation occurs at the transducer ends. A range of loads is applied by placing static weights on the lever arm.

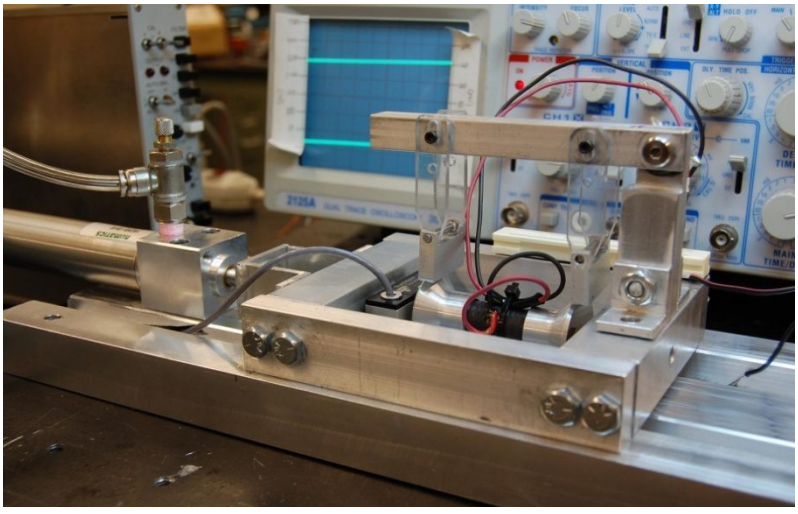

Fig.3. Experimental setup for measuring the average frictional force with and without ultrasonic vibrations at various macroscopic velocities.

The load cell, which measures the average frictional force between the transducer and guide rail, is connected to a signal conditioner to eliminate high frequency noise. We use a Data Physics ACE as the data acquisition system. It is set to record data at a frequency span of 80 Hz and block size of 256. The voltage and current driving the piezoelectric stack are monitored. By adjusting the flow valves on the air cylinder, we obtain the desired speeds. The velocity of the transducer (assumed constant) is measured from the time taken to traverse a known distance. The velocity of the ultrasonic vibrations is measured using a laser displacement sensor.

3. EXPERIMENTAL RESULTS

Tests were conducted for two different macroscopic velocities (0.038 m/s and 0.068 m/s) in order to assess the sensitivity of friction control to velocity ratio. The voltage applied to the stack is 6 V peak-to-peak at constant current amplitude of 2 A peak-to-peak. The frequency of the excitation signal is 40 kHz. The friction force is measured at no load and at loads of 1 N, 2 N, 5 N and 10 N.

Two sets of tests were conducted in order to quantify the effect of friction reduction. First, the actuator was run without the application of any excitation signal ("OFF" state). Next, the transducer was excited at t=3 sec to t=5 sec for case 1-low speed, and t=1.5 sec to 2.5 sec for case 2-high speed, using an external burst trigger mode ("OFF/ON" state). The results obtained are shown in Fig. 4 and Fig. 5.

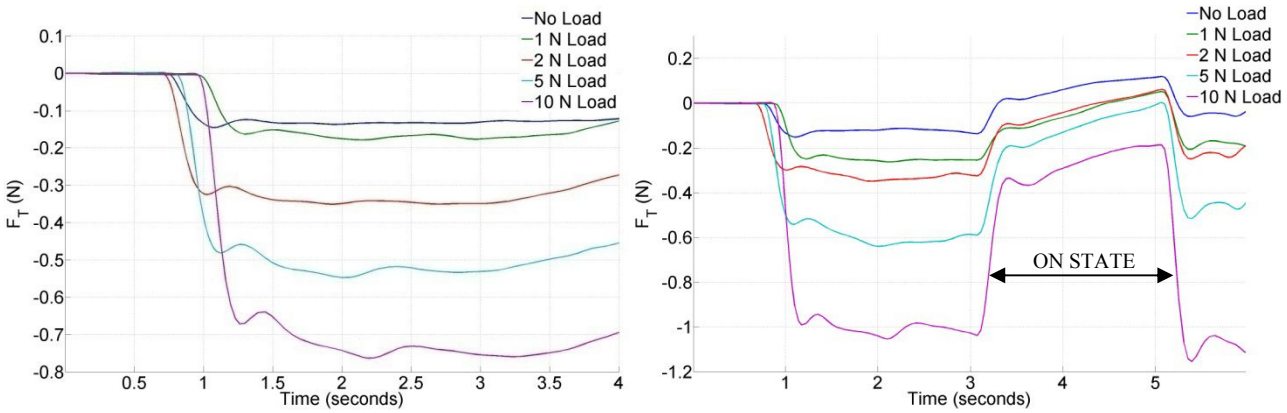

(a) (b)

Fig.4. Friction force measured at transducer velocity of 0.038 m/s in (a) "OFF" state and (b) "OFF/ON" state

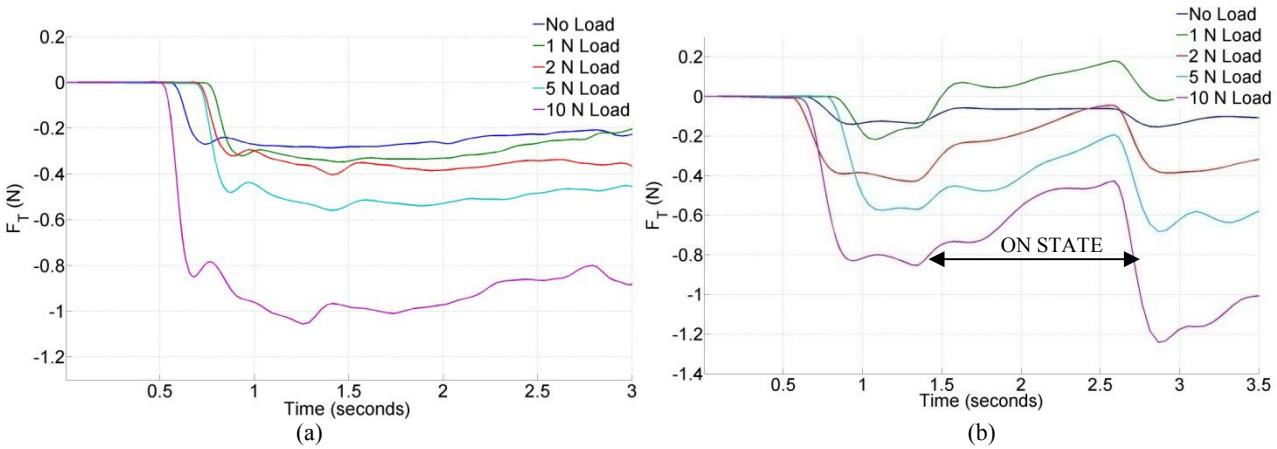

(a) (b)

Fig.5. Friction force measured at transducer velocity of 0.068 m/s in (a) "OFF state and (b) "OFF/ON" state.

Friction force in the OFF state is the dry friction between the transducer and guide rails. The load cell initially does not experience any force when the transducer is at rest. Once motion is initiated, there is a compressive force (with negative sign) on the load cell. This is the static friction force to be overcome to sustain relative motion. The compressive force measured by the load cell thereafter is the kinetic friction force. As the normal reaction (N=mg) increases with load (W), the friction force (μmg) also increases.

In the "OFF/ON state," i.e., when the PMN-PT stack is excited energized, ultrasonic vibrations along the direction of motion reduce the friction force at the interface. This creates a decrease in the compressive force on the load cell in Fig. 4 (b) and Fig. 5 (b). This trend is observed at both macroscopic speeds. However, the extent of reduction is observed to be greater in the case of low speeds. As the velocity ratio (ξ) increases, the effect of friction reduction decreases.

4. ANALYTICAL MODELING

In order to understand the mechanism of active friction control, two analytical models for friction control are considered: a) Coulomb friction model, and b) Dahl friction model.

4.1 Coulomb's friction model

Coulomb's model is based on the assumption that the interacting surfaces are ideally rigid. A free body diagram showing the various forces acting on the body is shown in Fig. 6.

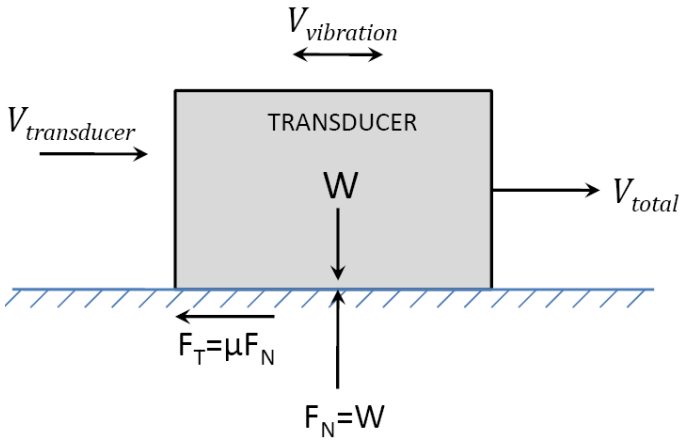

Fig.6. Coulomb's friction model.

For the transducer in motion, its velocity may be represented as the superposition of two velocities – a macroscopic velocity component ($v_{transducer}$) which is the velocity of the transducer, and a microscopic velocity component ($v_{vibration}$) which is the velocity of the vibration in the longitudinal direction,

$$v_{total} = v_{transducer} + v_{vibration}. \quad (1)$$

The microscopic component is a function of time, whereas the macroscopic component is a constant. Since we apply a harmonic excitation signal to the transducer, the displacements and velocities are harmonic. Then, $v_{vibration}$ may be written as

$$v_{vibration} = x_a\omega \cos \omega t = v_a \cos\omega t, \quad (2)$$

where x_a is the displacement amplitude of the vibration and ω is the excitation frequency (rad/s). Hence,

$$v_{total}(t) = v_{transducer} + v_a \cos \omega t. \quad (3)$$

Coulomb friction is defined by,

$$F_T = \mu mg\ sgn(v_{total}) = \mu mg\ sgn(v_{transducer} + v_a \cos \omega t), \quad (4)$$

where μ is the coefficient of kinetic friction between the surfaces and m is the mass of the body.

Assuming μ =0.2, the friction force is calculated at no load and at loads of 1 N, 2 N, 5 N and 10 N. It is assumed that 75% of the load is transferred to the transducer. The velocity $v_{transducer}$ is set at 0.038 m/s and 0.068 m/s. The applied excitation voltage is 6 V peak-to-peak and the excitation frequency is 40,000 Hz. The displacement amplitude is x_a = 0.3 μm. The amplitude of the vibration velocity is calculated to be 0.0683 m/s. Figures 7-9 show the calculated velocities and forces resulting from equations (3) and (4).

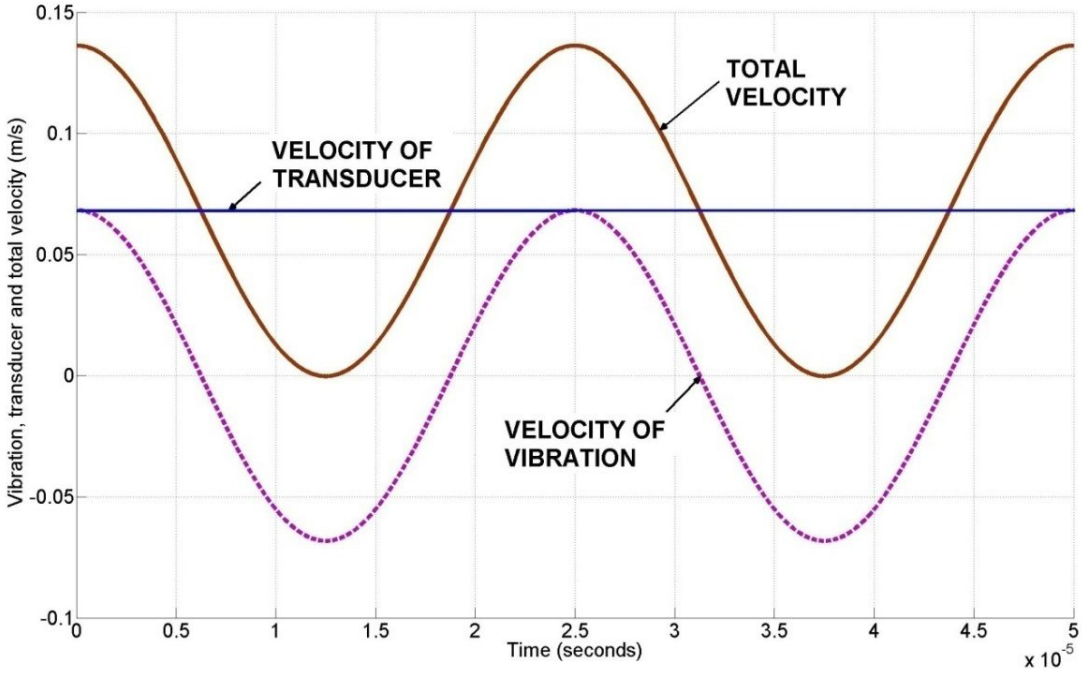

Fig.7. Time traces of transducer velocity, vibration velocity, and total velocity.

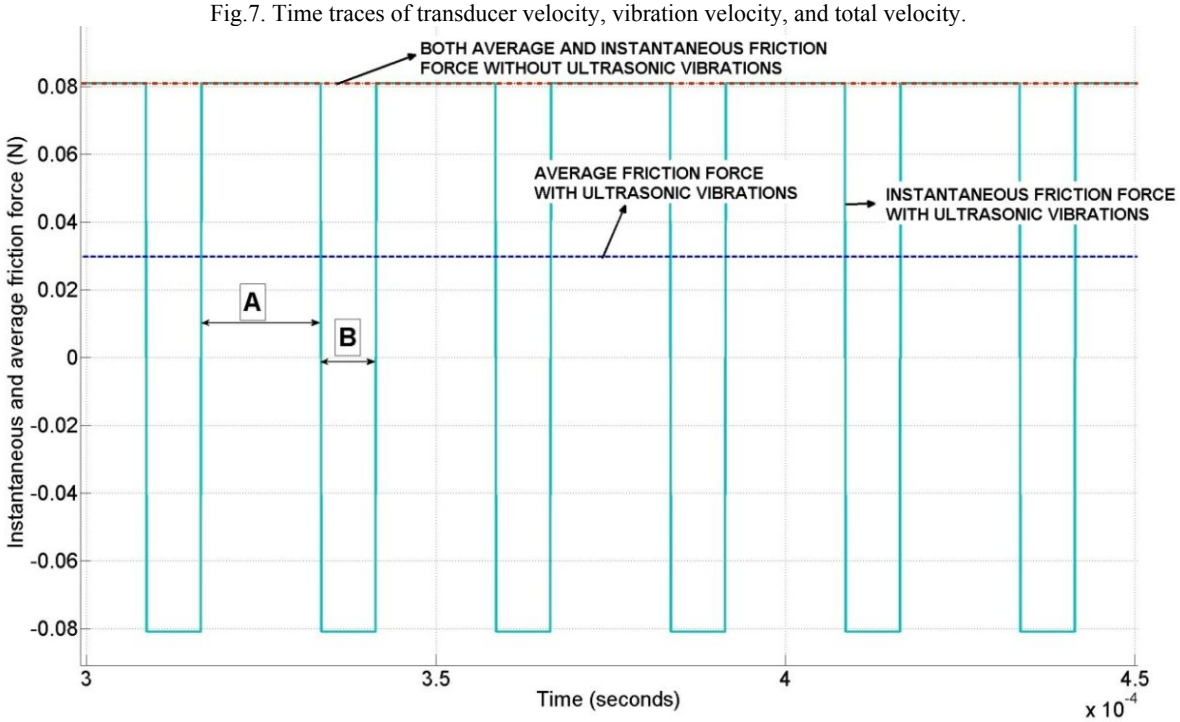

Fig.8. Effect of friction reduction in presence of ultrasonic vibrations as explained by Coulomb's model.

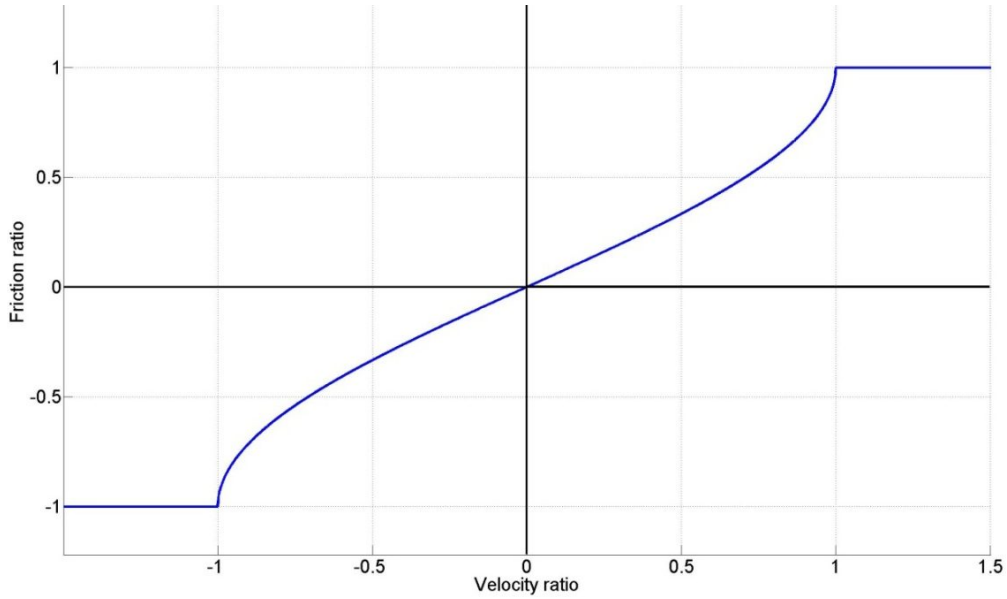

Fig.9. Ratio of average friction force with vibrations to average friction force without vibrations vs. velocity ratio (ξ), according to Coulomb's model.

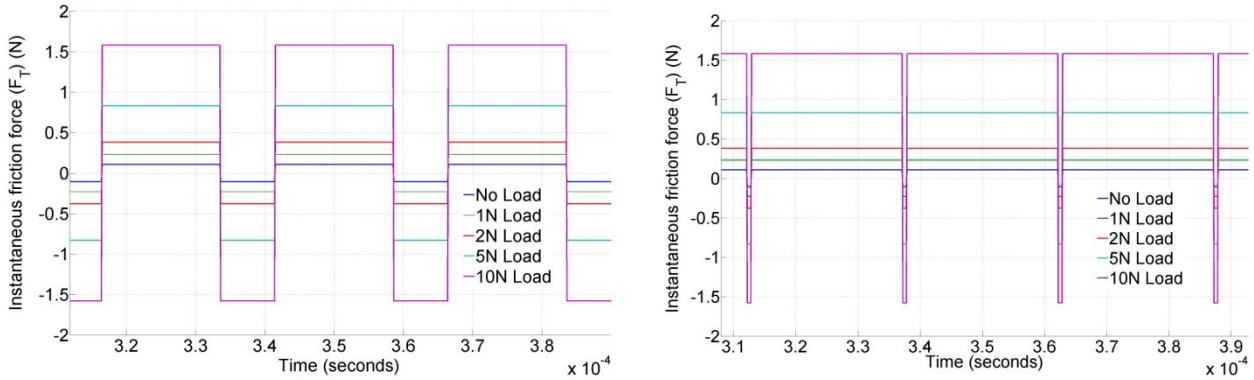

Fig.10. Instantaneous friction force versus time at different loads at transducer velocity of (a) 0.038 m/s and (b) 0.068 m/s.

In Fig. 8, A and B represent the widths of the pulsating force as the vibration velocity changes sign. As the velocity ratio increases, B decreases, and the effect of friction reduction diminishes, as seen in Fig. 10(b). When the macroscopic and microscopic velocities become equal to each other, there is no friction reduction and the instantaneous friction force becomes equal to μmg. When the velocity ratio is close to zero, the sign is dominated by the vibration velocity and the instantaneous force becomes equal to a rectified cosine. The width A becomes nearly equal to B and the average friction force approaches zero (maximum friction reduction).

3.2 Dahl's friction model

Dahl's model is based on the assumption that during sliding motion, there are continuous deformations, both elastic and plastic, at the area of contact. The real area of contact between two surfaces is less than the apparent area. This is because surfaces are not perfectly smooth and the actual contact points are asperities that exist on both surfaces. During sliding, the asperities undergo plastic and elastic deformation. Work is done to break the adhesive bonds between the asperities. The classical Coulomb's model does not consider this behavior.

In Dahl's model the asperities present on the interacting surfaces are modeled as micro-springs. When a tangential load is applied, a force is required to overcome the spring force exerted in the direction opposing motion. Once the force is large enough, the contact is broken and sliding takes place.

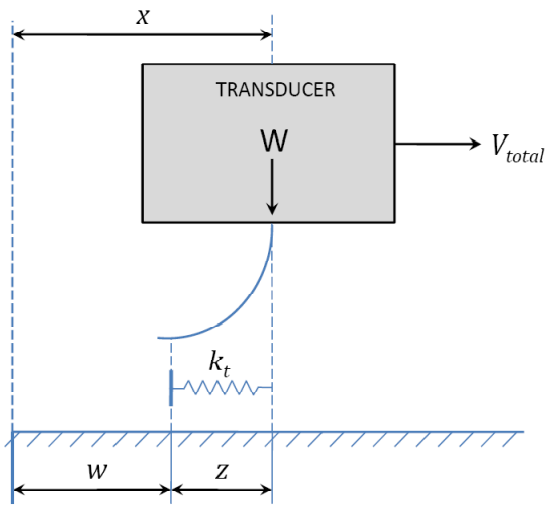

Fig.11. Dahl's friction model.

According to Dahl's model [6], the total displacement $\boldsymbol{x}$ of the rigid body can be broken down-an elastic z and plastic w component,

$$x = z + w. \tag{5}$$

The elastic component is related to the elastic deflections of the asperities in the tangential direction. The friction force F_T is then given by,

$$F_T = k_t z, \tag{6}$$

in which k_t is the tangential contact stiffness. Based on analysis carried out in [12], k_t is assumed to be 0.056 N/μm.

The deflection is described with a differential equation,

$$\frac{dz}{dt} = v_{total}\left(1 - \frac{k_t z}{\mu mg} sgn(v_{total})\right)^{\alpha}. \tag{7}$$

Here, α is a parameter that defines the shape of a curve describing the dependence of the tangential deflections. For brittle materials, $\alpha < 1$ and for ductile materials, α is ≥ 1 [12]. In our case, we have considered $\alpha = 1$. To calculate the deflection, z and frictional force F_T, a MATLAB *Simulink* model is developed (Fig. 12). The instantaneous and average friction force calculated in this manner is shown in Fig. 13.

3.3 Comparison of Coulomb and Dahl friction models with experimental data

In Coulomb's model, the instantaneous friction force changes its vector sign continuously in order to obtain a reduction in the average friction force. In Dahl's model, the instantaneous friction force does not change its vector sign. Instead, it gradually changes its direction and then starts to grow in the opposite direction. A comparison of the instantaneous friction forces in both models for a given load and velocity is shown in Fig. 17 (a). Both models depend on the velocities of the sliding objects. The friction ratio varies with the velocity ratio for both models as shown in Fig. 17(b). It can be observed that for a given velocity ratio, the theoretical percentage reduction can yield different results depending on the model chosen.

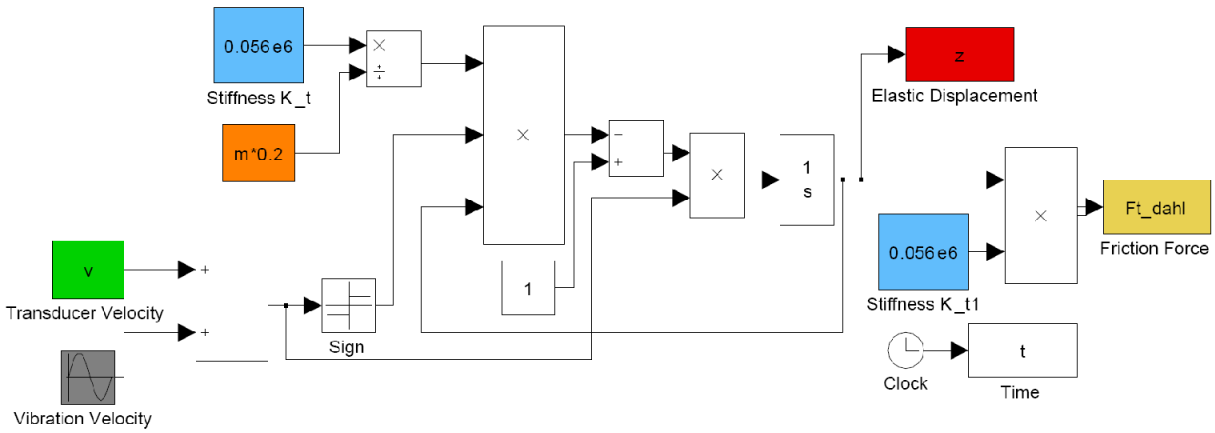

Fig.12. *Simulink* model for Dahl's friction model.

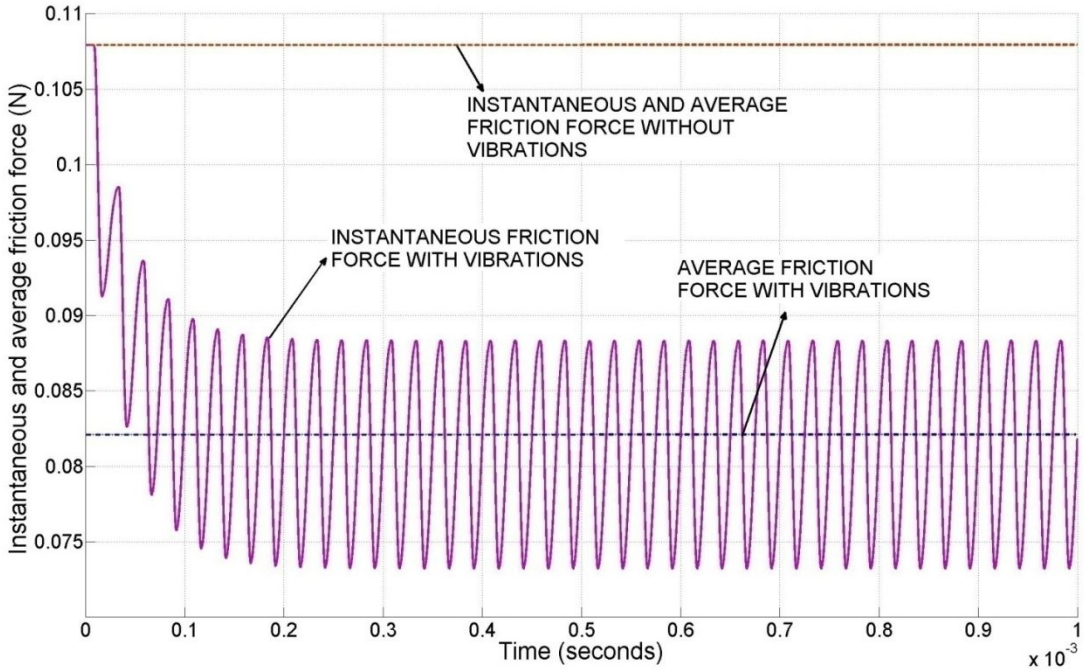

Fig.13. Effect of friction reduction in presence of ultrasonic vibrations as described with Dahl's model.

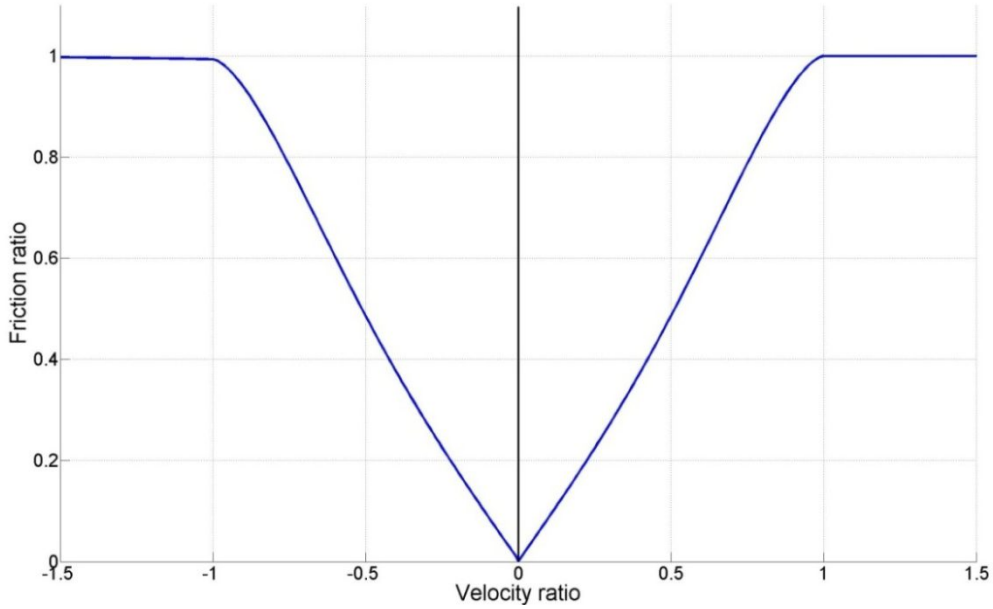

Fig.14. Ratio of average friction force with vibrations to average friction force without vibrations vs. velocity ratio (ξ), as described with Dahl's model.

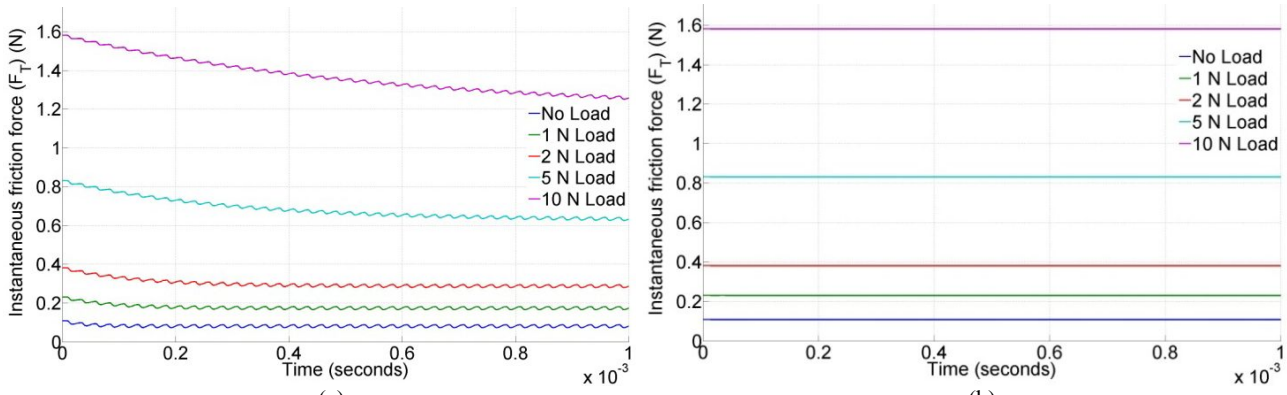

(a) (b)

Fig.16. Instantaneous friction force versus time at different loads at transducer velocity of (a) 0.038 m/s and (b) 0.068 m/s.

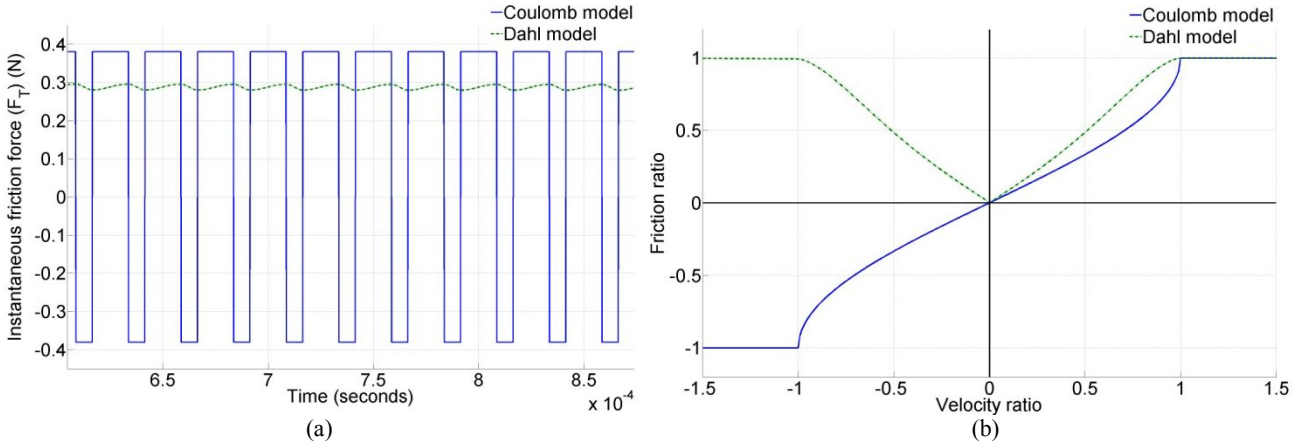

(a) (b)

Fig.17. (a) Comparison of instantaneous friction force using Coulomb and Dahl models at a given load and velocity. (b) Comparison of friction ratio vs. velocity ratio using Coulomb and Dahl models.

Table 2. Comparison of experimental results with analytical models for transducer velocity of 0.038 m/s. Velocity of transducer= 0.038 m/s, ξ = 0.56. Voltage = 6 V p-p @ 40 kHz.											
Load (N)	**W (N)**	**μmg (N)**	**F_t(N)**	**F_t^* (N)**	**μ = F_t/W**	**μ^* = F_t^*/W**	**F_t^*(Coulomb) (N)**	**F_t^*(Dahl) (N)**	**%Reduction (Experiment)**	**%Reduction (Coulomb)**	**%Reduction (Dahl)**
0	0.540	0.108	0.11	0.035	0.20	0.06	0.0397	0.0821	68.18	63.21	23.92
2	1.902	0.380	0.365	0.097	0.19	0.05	0.1402	0.2999	73.42		21.15
5	4.155	0.831	0.622	0.198	0.15	0.05	0.3059	0.6849	68.17		17.57
10	7.905	1.581	1.054	0.368	0.13	0.05	0.5819	1.3737	65.09		13.11

Table 3. Comparison of experimental results with analytical models for transducer velocity of 0.068 m/s. Velocity of transducer = 0.068 m/s, ξ = 1. Voltage = 6 V p-p @ 40 kHz.											
Load (N)	**W (N)**	**μmg (N)**	**F_t (N)**	**F_t^* (N)**	**μ = F_t/W**	**μ^* = F_t^*/W**	**F_t^*(Coulomb) (N)**	**F_t^*(Dahl) (N)**	**% Reduction (Experiment)**	**% Reduction (Coulomb)**	**% Reduction (Dahl)**
0	0.540	0.108	0.112	0.087	0.18	0.09	0.1019	0.1079	22.32	5.57	0.01
2	1.902	0.380	0.383	0.292	0.18	0.09	0.3596	0.3809	23.76		-0.15
5	4.155	0.831	0.564	0.544	0.15	0.08	0.7845	0.8309	3.58		0.00
10	7.905	1.581	0.813	0.793	0.12	0.07	1.4926	1.581	2.46		0.00

3.4 Effect of controlling parameters

It is observed that the static contact pressure, velocity, voltage and frequency are the primary controlling parameters for active friction control. The effect of these parameters is discussed below:

Effect of load - Experimental data shows that at the lowest speed the percentage reduction in friction force is relatively independent of load (for the loads considered). At the highest speed tested, there are two well defined reduction values depending on load. Coulomb's model provides a calculation of the percentage reduction which is independent of the applied load. At the lowest speed, Dahl's model is dependent on the applied load as the percentage reduction in friction decreases with an increase in normal load.

Effect of velocity - Coulomb's equation is not a function of the actual velocities but only of the velocity ratio. Thus, irrespective of the magnitudes, Coulomb's equations take into account only the vector sign of the total velocity. On the other hand, Dahl's model is dependent on the magnitudes of the velocities and not on the velocity ratio. For the same velocity ratio but higher velocities, Dahl's model gives a much higher percentage reduction. For low transducer and vibration velocities, Dahl's model does not correlate well with experimental results. As the velocity ratio approaches unity, the effect of friction reduction vanishes.

Effect of voltage and frequency - An increase in voltage increases the displacement amplitude of the stack and an increase in cyclic frequency increases the amplitude of the vibration velocity. This tends to reduce the velocity ratio. In theory, a much higher percentage reduction in friction can be obtained by increasing the applied voltage or frequency. However, the maximum voltage that can be applied is limited by the properties of the piezoelectric material. The frequency is limited by the half wavelength operation of the stack. Since maximum displacement is created at the end points at the transducer's resonant frequency, this parameter is a design constraint.

3.5 Discussion on experimental data

The experimental data at high transducer velocities shows inconsistencies, which are most likely due to fluctuations arising from the experimental setup. The aluminum shells and guide rail abrade during sliding, thus slightly changing the frictional properties after each test run. At high velocities, the assumption of constant transducer velocity may not necessarily hold. Since we use a pneumatic cylinder to drive the transducer, there is a brief period when the cylinder accelerates and reaches a steady-state velocity. Over a short distance, obtaining a constant high velocity is therefore a challenge with this setup. As part of ongoing work, we are improving the experimental setup to obtain repeatable and consistent data at higher loads and higher velocities which is of primary importance in commercial applications.

5. SUMMARY

This study complements previous research showing that ultrasonic vibrations superimposed parallel to the macroscopic motion of a sliding object can reduce friction. The extent of friction reduction depends on the velocity ratio (ratio of the velocity of the sliding body to the velocity of ultrasonic vibrations). The effect is more pronounced for low velocity ratios. In the presence of an additional normal load, the friction force increases proportionally. The percentage change in friction force is independent of the load in case of the Coulomb friction model, whereas the opposite is the case in Dahl's model. For low velocity ratios, experimental results can be correlated with Coulomb's model. For the same velocity ratio but higher velocity magnitudes, Dahl's model suggests a higher percentage reduction in friction. As the velocity ratio approaches unity, the effect of friction reduction vanishes. Active control of friction using ultrasonic vibrations would help improve the performance, efficiency, and lifetime of sliding mechanisms in automotive applications. Future work will focus on the application of this research to seat belt systems.

ACKNOWLEDGMENT

Financial support for this research was provided by the Smart Vehicle Concepts Center (www.SmartVehicleCenter.org), a National Science Foundation Industry/University Collaborative Research Center.

REFERENCES

[1] B.Bhushan, "Introduction to Tribology," ISBN 0471158933, John Wiley and Sons, 2002.
[2] T. Hesjedal, and G. Behme, "The origin of ultrasound-induced friction reduction in microscopic mechanical contacts," *IEEE Trans. Ultrasonics, Ferroelectrics, and Frequency Control*, Vol.49, No.3, pp. 356-364, 2002.
[3] W. Littmann, H. Storck, and J. Wallaschek, "Sliding friction in the presence of ultrasonic oscillations: superposition of longitudinal oscillations," *Archive of Applied Mechanics*, 71, pp. 549-554, 2001.
[4] H. Storck, W. Littmann, J. Wallaschek, and M. Mracek, "The effect of friction reduction in presence of ultrasonic vibrations and its relevance to traveling wave ultrasonic motors," *Ultrasonics*, 40, pp. 379-383, 2002.
[5] W. Littmann, H. Storck, and J. Wallaschek, "Reduction in friction using piezoelectrically excited ultrasonic vibrations," SPIE's 8th international Symposium on Smart Structures and Materials, Vol. 4331, pp. 302-311, 2001.
[6] M. Leus and P. Gutowski, "Analysis of longitudinal tangential contact vibration effect on friction force using Coulomb and Dahl models," *Journal of Theoretical and Applied Mechanics*, 46, pp. 171-184, 2008.
[7] K. Cunefare, and A. Graf, "Experimental active control of automotive disc brake rotor squeal using dither," *Journal of Sound and Vibration*, 250(4), pp. 579-590, 2002.
[8] M. Neubauer and R Oleskiewicz, "Brake squeal control with shunted piezoceramics – efficient modeling and experiments," Proceedings of IMechE, Vol. 222, Part D: J. of Automotive Engineering, 592, pp. 1141-1151, 2008.
[9] J. Badertscher, K. Cunefare, and A. Ferri, " Braking impact of normal dither signals," *Journal of Vibration and Acoustics*, Vol. 129, Transactions of the ASME, pp. 18-23, 2007.
[10] P. Hagedorn, and U. von Wagner, "Smart pads": a new tool for the suppression of brake squeal?," Proceedings of XXIV μ—Kolloquium, B. Breuer (Ed.), VDI-Bericht, Vol. 575, 2003.
[11] M. Michaux, A. Ferri, and K. Cunefare, "Effect of tangential dither signal on friction induced oscillations in an SDOF model," *Journal of Computational and Nonlinear Dynamics*, 2, pp. 201-210, 2007.
[12] C.C. Tsai and C.H. Tseng, "The effect of friction reduction in the presence of in-plane vibrations," *Archive of Applied Mechanics*, 75, pp. 164-176, 2005.
[13] P. Hagerdorn, D. Hochlenert, and R. Dunlop, "Piezoelectric sensors and actuators in disk brakes," Proceedings of 5th International Workshop on Structural Control and Health Monitoring, 2005.
[14] T. Jearsiripongkul, and D. Hochnelert, "Disc brake squeal- modeling and active control," IEEE Conference on Robotics, Automation and Mechatronics, pp. 1-5, 2006.